EFFECTS OF FABRIC ARCHITECTURAL HETEROGENEITIES ON EFFECTIVE AND SATURATED PERMEABILITIES IN RTM

C. Binétruy and J. Pabiot

Ecole des Mines de Douai, Technology of Polymers and Composites Department
941 Rue Charles Bourseul, 59508 Douai Cedex, France

SUMMARY : The purpose of this work is to investigate the effects of fabric architectural heterogeneities on the effective and the saturated in-plane permeabilities of single and multi-layers preforms. To do this, a glass random mat, unidirectional and bidirectional woven glass fabrics have been used to generate different structural heterogeneities and to introduce several embedded length scales into the flow. The proposed model takes into account the large-scale heterogeneity of the reinforcements to determine the hierarchy of local flows by searching possible transverse flows occuring from inter-tow spaces to intra-tow gaps or from certain layers into adjacent layers. Flow vizualizations and permeability characterizations show complicated trend which are simulated with a quite good accuracy by the model. Significant time-dependent effects are observed for thick architecturally complex materials.

KEYWORDS : Resin Transfer Molding, Mold Filling, Fabric Architectural Heterogenity, Saturated Permeability, Effective Permeability, Model.

INTRODUCTION

Resin Transfer Molding (RTM) is a process in which complex shape composite parts can be produced by infiltrating architecturally-complex fibrous materials with a liquid resin. To optimize the filling process, flow simulations are often used. It is acknowledged that the accuracy of these simulations depends strongly upon the reliability of the input preform permeability values. There are different techniques to measure permeability values : in one or two dimensional flow, in steady or unsteady condition and with constant pressure or constant flow rate driven flow. The unsteady flow condition is in accordance with the actual RTM process and flow extents have to be recorded to deduce effective permeability values (K^{eff}). For this purpose, this method requires the use of specific apparatus including clear molds or multiple pressure sensors or another non-destructive techniques. On the other hand, the measurement of saturated permeabilities (K^{sat}) in steady flow condition is easier to process and may be a more attractive way to characterize the flow behavior inside preforms. Altougth there is an important distinction to be made between these two quantities, they are often mistaken in practice. The different sources involved in their difference are known as fluid properties, surface tension effects and materials architecture. Wicking effets should produce an apparent enhancement in the effective permeability espacially at the beginning of the filling. This phenomenon has been observed with non crimp stitch bonded bi-directional

materials [1] and with random mats [2]. Air bubbles generated during the preform filling may be trapped between adjacent tows or displaced as the fluid front advances. Depending on wether bubbles are flushed out the fibrous medium or remains trapped during the saturated regime, dry permeability may be higher than steady state permeability [3].
Another physical explanation is the influence of the fibrous material architecture. One of the most important microstructural characteristic of many preforms used in RTM is their heterogeneity as at least three length scales can be defined : a macroscopic scale which corresponds to the observation scale in practice (associated to the dimension of the composite part), a mesoscopic scale where inter-tow spaces (macropores) are defined and a microscopic scale where intra-tow volumes (micropores) are located. In processing resin flows through both Macropores and micropores and each of which contributes to the overall saturated and effective permeabilities of the preform. A large-scale architectural heterogeneity will conduct to complicated trends since the effective permeability can be lower than the saturated value at the beginning of the preform impregnation, proceeded to increase to a level rougly 30% to 50% above the saturated value [4]. The relative time scales of the tow impregnation process and the macroscopic flow seems determine if the ratio K^{eff} / K^{sat} is over one or not. In spite of many efforts to model this complex behaviour [5], additional work is necessary to capture the effect of material heterogeneity in term of effective permeability, particulary by analysing all possible length scales associated to the fibrous medium to rebuild the real fluid flow path.

This work adresses the issue of the effects of fabric architectural heterogeneity on both theoretical and experimental permeability differences. The originality of this approach is the considering of the overall length scales embedded in the preform to model the flow behavior and to derive effective values.

MODEL

The proposed model includes a first step in which local flow resistances at the tow-scale are numerically calculated, the second step deals with the development of the hierarchy of local flows over increasing length and time. A specific averaging scheme has been developed to calculate an effective average permeability. Because of the large difference in permeability existing between inter-tow spaces (Macropores) and intra-tow spaces (micropores), the tow impregnation is mainly controled by the flow in the transverse direction. The resulting flow front presents a pointed meniscus shape (figure 1) whose length (Δz) has been modeled in a previous study [6-7]. To derive an effective permeability value, this pointed front is transformed into the equivalent front depicted in figure 1 to get a rectilinear one-dimensional flow. To do this, the area A actually impregnated in processing is displaced towards the B location.

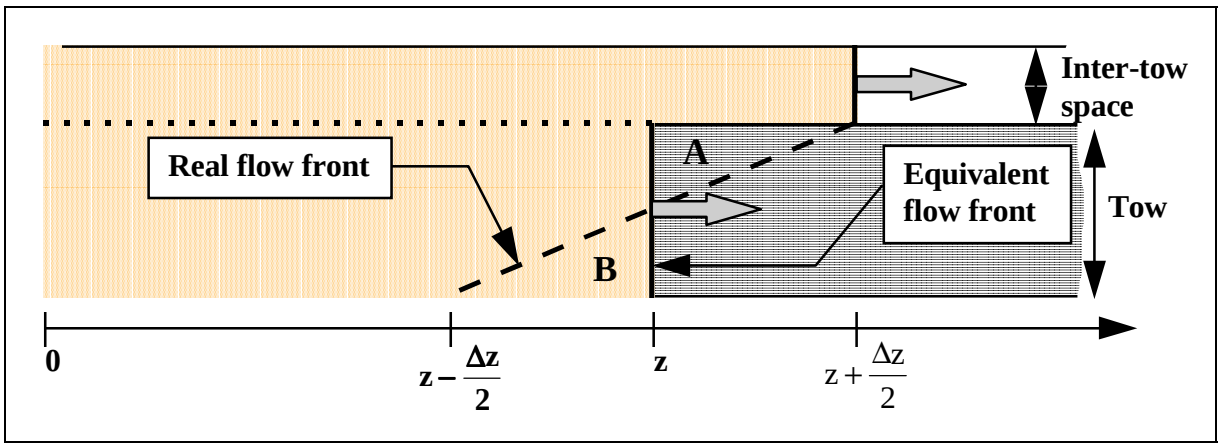

Fig. 1 : Transformation of the real flow front in micropores into an equivalent flow front.

The total volumetric flow rate is known from the mass balance :

$$Q_T = Q_M + Q_m \tag{1}$$

The overall effective permeability $\overline{K}^{eff}$ in the flow direction (z) and the Macropores permeability K_M^{eff} can be defined with the Darcy's law as follows :

$$\overline{K}^{eff} = \frac{\mu z Q_T}{P.(A_M + A_m)} \tag{2}$$

$$K_M^{eff} = \frac{\mu(z + \Delta z/2)Q_M}{P.A_M} \tag{3}$$

By integrating the Darcy's law and assuming a quasi-steady-state situation, the equivalent intra-tow permeability (figure 1) can be related to the effective inter-tow permeability by :

$$\left(\frac{z + \Delta z/2}{z}\right)^2 = \frac{K_M^{eff}}{K_m} \tag{4}$$

The volumetric flow rate through the intra-tow spaces is expressed in function of the Macropores flow as follows :

$$\frac{Q_m}{A_m} = \frac{P.K_M^{eff}\left(\frac{z}{z + \Delta z/2}\right)^2}{\mu.z} \tag{5}$$

Finally the overall effective permeability in the flow direction (z) is given by :

$$\overline{K}^{eff} = \frac{K_M^{eff}}{(A_M + A_m)\left(1 + \frac{\Delta z}{2z}\right)}\left(A_M + \frac{A_m}{1 + \frac{\Delta z}{2z}}\right) \tag{6}$$

One can notice that the $\overline{K}^{eff}$ value depends on the flow front position as long as the order of magnitude of the ratio $\frac{\Delta z}{2z}$ is significant. It is a first time-dependent effect. As the flow front advances the relationship (6) can be simplified since :

$$\overline{K}^{eff} \to K_M^{eff} \quad \text{as} \quad \frac{\Delta z}{2z} \to 0 \tag{7}$$

A methodology has been developped in a previous work to calculate the effective permeability of the inter-tow spaces as a function of its geometry and the transverse permeability of the bordering tows [8].

The proposed relationship is :

$$K_M^{eff} = K_M^{sat}\left(1-\left(\frac{K_m^t}{K_M^{sat}}\right)^{\frac{1}{8}}\right)^2 \qquad (8)$$

To achieve this a new boundary condition at the tow surface and limited only near the flow front region has been proposed. This first kind of interaction occuring at the tow scale has been completed with interactions between Macropore flows. Indeed within heterogeneous fibrous media, the Macropores size distribution may be wide, and finite flows in the transverse direction may affect the impregnation of most resistant inter-tow ducts, decreasing the expected lag distance between regions of different permeabilities. A specific model has been proposed to account for this mechanism [9]. It requires the knowledge of the different data presented in figure 2 which are the Macropores permeabilities (K_{Mi}, K_{Mj}), both axial and transverse tow permeabilities (K_m^a, K_m^t) and the distance between the Macropores in the transverse direction (e_{ij}). This explains why it is important to achieve the geometric inspection of the structure to deduce the pore size distribution. It is the first step of the global numerical procedure summarized in figure 3.
The saturated permeability of Macropores are numerically determined by solving the continuity and the creep motion momentum equation with a no slip condition along the tow boundary. A Ritz-Galerkin method is used to do this. The overall saturated permeability is calculated using the simple weighted arithmetic average as there is no transverse flow.
As soon as the effective permeabilities of the inter-tow spaces are determined, the hierarchy of local flows is calculated by considering first the more permeable Macropores and their influence over increasing in-the-thickness distance and time. It is a second time-dependent effect. Afterwards the flow front position in each layer is updated and the overall effective permeability is derived by means of the above averaging scheme. Here a layer refers to a part of the fibrous network across the thickness which has the same in-plane permeability in the flow direction. A typical example of the difference between a saturated flow and the impregnation of a dry fibrous structure is sketch in figure 4.

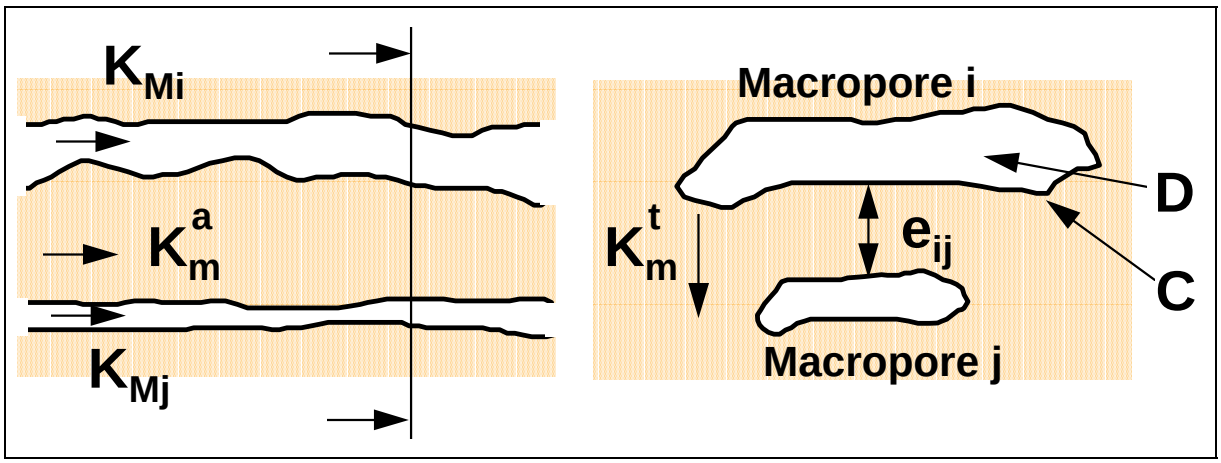

Fig.2: Schematic description of the heterogeneous fibrous medium and the different data required to model the interactions between the inter-tow flows

This numerical procedure allows one to investigate the influence of the fabric architectural heterogeneities on the saturated and effective permeabilities. In order to examine the accuracy

of the proposed model and its ability to predict the difference between saturated and effective permeabilities, experimental results are compared to the calculated values. In this purpose we have selected fibrous materials which cover different cases of length scale.

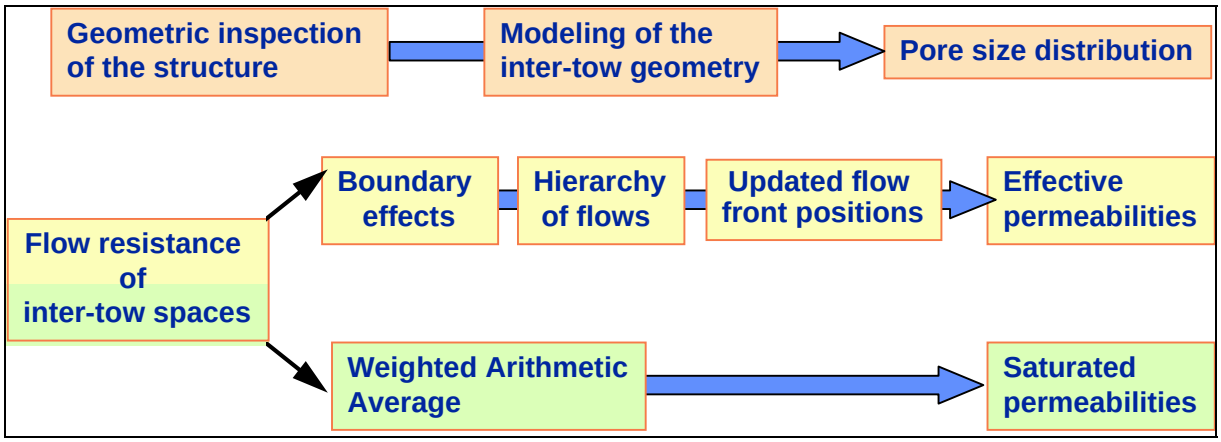

Fig. 3 : Flowchart of the numerical procedure to predict both saturated and effective permeabilities and to investigate the influence of the fabric architectural heterogeneities on the flow mechanism

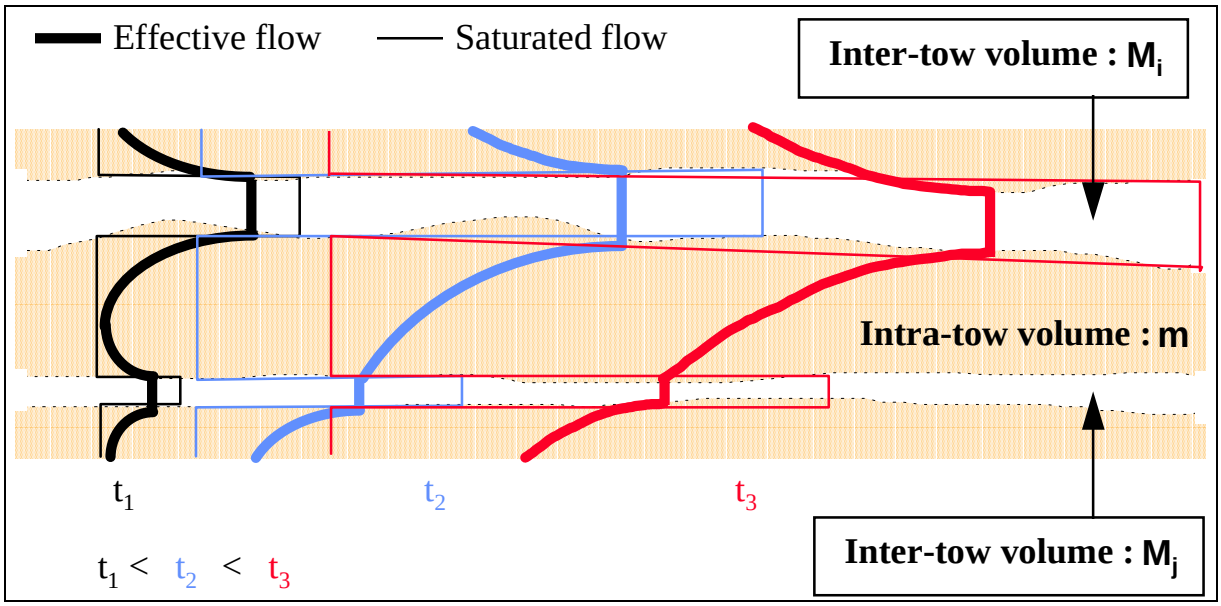

Fig.4 : Typical tow-level structural heterogeneity encountered in woven fabrics which may give rise to significant time-dependent effects

EXPERIMENTS

Materials

A glass continuous fiber mat (CFM) of 450 g/ m^2 referenced U750 and manufactured by VETROTEX, an unidirectional glass woven fabrics (UD) of 420 g/ m^2 referenced SO 120 and manufactured by CHOMARAT and a bidirectional 3x1 plain weave glass fabric (BD) of 580 g/ m^2 manufactured by CHOMARAT are used to create different length scales associated to architectural heterogeneities.

The following stacking sequences have been studied : one layer of the unidirectional woven fabric (referenced 1 UD), the $[0,90]_6$ preform made with the unidirectional woven fabric (referenced 12 UD), 9 layers of bidirectional fabric and 5 layers of mat (referenced CFM/BD), 12 layers $[0,90]_6$ of unidirectional woven fabric and 5 layers of mat (referenced

UD/CFM). Micrographic inspections have been performed on composite manufactured with these preforms to determine the pore size distribution.
Measurements are carried out with a mineral oil referenced Tellus SX 46 and manufactured by SHELL. Its viscosity at room temperature is 0.1 Pa.s. The preform properties used for the calculation are summarized in table1. Permeabilities of each reinforcement were determined in the 1-D unsaturated flow geometry.

	1 layerUD	**12 layers UD $[0,90]_6$**	**9 layers BD**	**5 layers CFM**
K_z^{eff} (m^2)	$2\ 10^{-10}$	$8\ 10^{-11}$	$2\ 10^{-10}$	$2\ 10^{-9}$
K_x^{eff} (m^2)	$2\ 10^{-13}$ (tow permeability)	10^{-12}	10^{-11}	$3\ 10^{-9}$
Fiber content inside the mold (%)	54	52	54	24
Thickness inside the mold (mm)	0.3	3.7	3.7	3.6

Table 1 : Materials properties

Experimental setup

In the experimental part of this study both longitudinal effective and saturated permeabilities are measured by means of a 0.3 x 0.3 m^2 flat clear mold set on a balance in the vertical upward position. Injection are conducted at contant pressures with the selected mineral oil in the one-dimensional flow geometry, the top and bottom flow extents, the inlet and outlet pressures and the injected mass being recorded. Inlet pressures are chosen so as to generate flow front velocities over than 1 mm/s. In this situation surface effects can be neglected [6]. The schematic description of the experimental setup is given in figure 5a. From the inlet flow initiation up the saturation of the preform (figure 5b), the flow front progression observed on both top and bottom of the mold, the constant inlet pressure and the injected fluid mass are monitored at regular time intervals to calculate K^{eff} with the above presented model. After the reinforcement is continued to be filled to reach a steady-state processing condition at which time the pressure gradient and the injected fluid mass are recorded to determine K^{sat} (figure 5c).

RESULTS AND DISCUSSION

Before the flow visualization stage, multi-layers preforms have been characterized in compression so that in-situ volume fractions and thickness of the different stacked layers are known. Figure 6 to 9 present the comparison between the experimental results and preditive calculations for the selected preforms in term of the dimensionless ratio K^{eff}/K^{sat}. As expected, the ply of unidirectional woven fabric exhibits a simple trend expressed by the ratio $K^{eff} / K^{sat} = 1$. This structure characterized by two distinct homogeneous pore families (Macropores and micropores) illustrates an instantaneous control of the the tow impregnation by the Macropores flow. However an enhancement in the effective permeability is noticed at the beginning of the impregnation owing to wicking effects.

On the contrary, the Macropores size distribution of the 12 UD material was found to be heterogeneous since the more open inter-tow regions are four times as permeable than the less one. This may be due to the local fiber rearrangement when the material is compressed during the mold closing step. These different Macropores ducts are separated by compacted tows and the rate of tow impregnation has been compared to the time scale of the front

progression in the adjacent Macropores. Along approximately the first third of the total flow extent, the transverse flows are limitated to the tow impregnation and some finite flows in the transverse direction start to affect the impregnation of the more resistant inter-tow ducts. Here the Macropores ducts can be viewed as "parallel" channels like in the saturated flow condition, but in the case of the unsaturated flow, the tow impregnation decreases the flow velocity in Macropores [10]. As the front advances, the more open Macropores will control the more resistant macropores channels and depending on the mold length, they may control the entire preform filling. The longer the mold length, the more marked is this trend (figure 7). It explains why just after the flow initiation, there was a decrease of K^{eff} below K^{sat} followed by an increase back over K^{sat}.

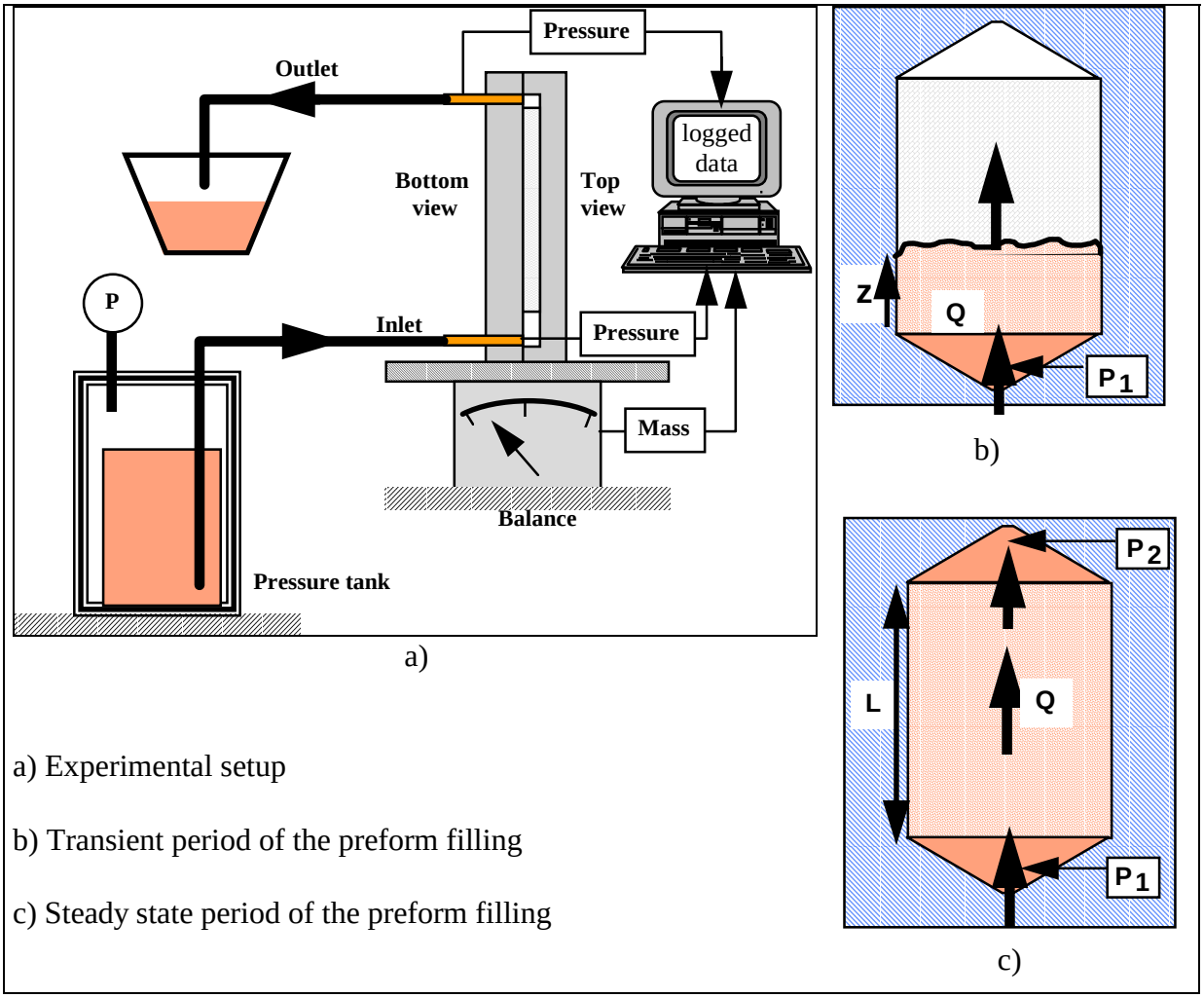

a) Experimental setup

b) Transient period of the preform filling

c) Steady state period of the preform filling

Fig.5 : Schematic description of the experimental setup

The same analysis can be done to explain the trend depicted in figure 8. Due to the much greater in-plane permeability of the mat, its impregnation starts out relatively quickly compared to the filling of the BD layers, but slows due to the transverse flow out the mat into the BD material. On the contrary this transfer of fluid induces an increase of the flow front impregnation in the BD layers, which means that the more permeable layers (Mat) will control gradually the whole preform impregnation. Good qualitative and quantitative agreements are observed between the calculations and the experimental data. Wicking effects have been measured for this material.

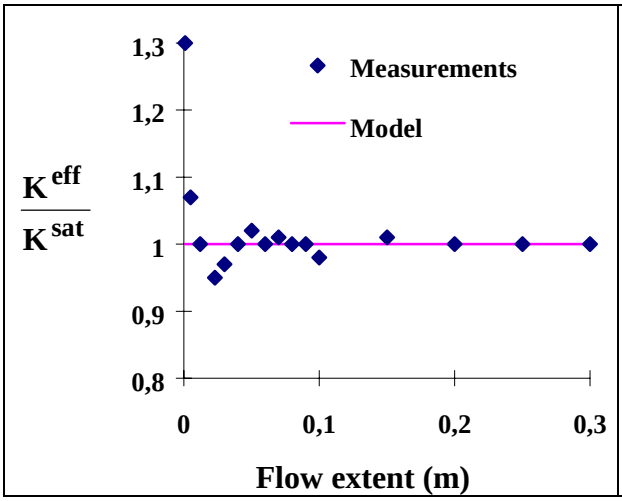

Fig.6 : Comparison of the experimental and numerical evolutions of the ratio K^{eff}/K^{sat} for one layer of unidirectional woven fabric (1 UD)

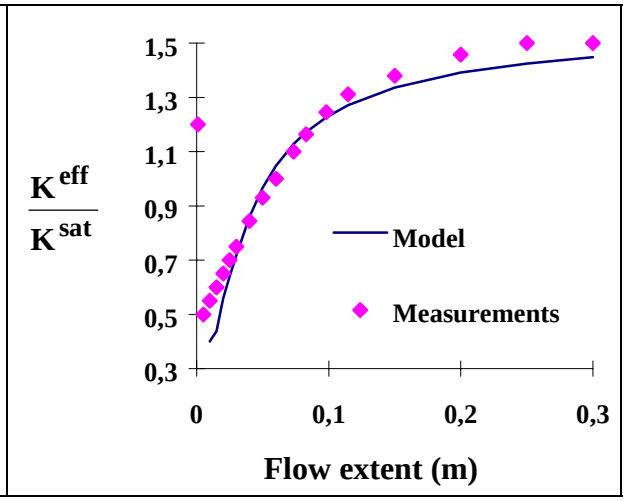

Fig.7 : Comparison of the experimental and numerical evolutions of the ratio K^{eff}/K^{sat} for the $[0,90]_6$ preform made with unidirectional woven fabric (12 UD)

It is interested to note that the trend depicted in figure 9 for the UD/CFM material differs from the previous material. In this case, the low through-the thickness permeability of the 12 UD layers (10^{-12} m^2) delays the control of the preform impregnation by the mat.

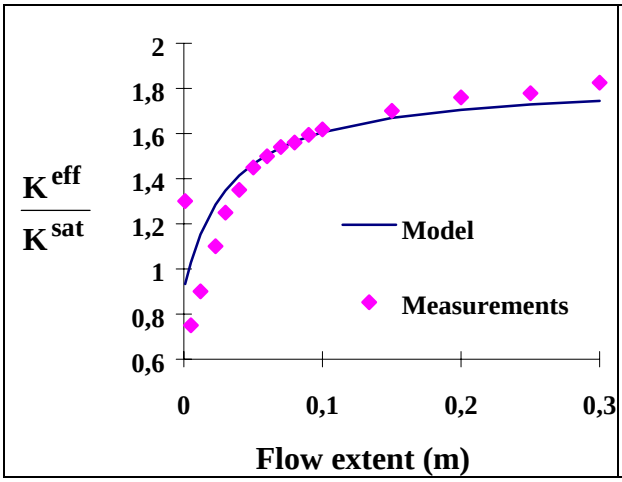

Fig.8 : Comparison of the experimental and numerical evolutions of the ratio K^{eff}/K^{sat} for 9 layers of bidirectional fabric (3.7 mm thick) and 5 layers of mat (3.6 mm thick)
(CFM/BD)

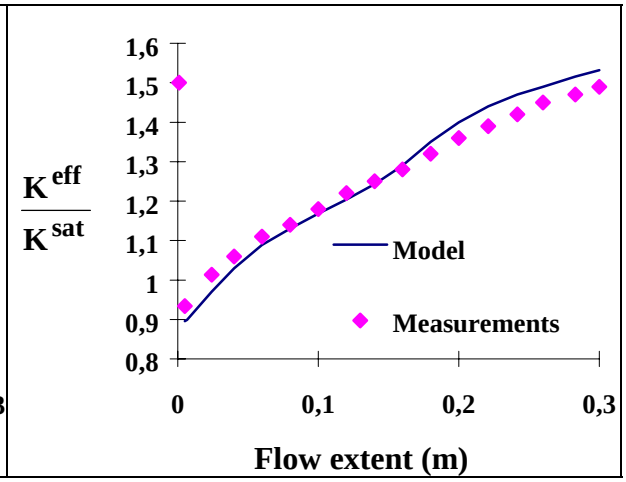

Fig.9 : Comparison of the experimental and numerical evolutions of the ratio K^{eff}/K^{sat} for the preform made with 12 layers $[0,90]_6$ of unidirectional woven fabric (3.7 mm thick) and 5 layers of mat (3.6 mm thick)
(UD/CFM)

In figure 10 are summarized the experimental data gathered in this work. Evolutions of the ratio K^{eff}/K^{sat} is clearly related to the relative thickness and the transverse permeabilities of layers, the total length of the mold and the number of length scales embedded in preforms.
For materials with several embedded length scales, large molds are required to fully characterize the flow behavior and to get steady-state values of effective permeabilities. These results show that significant mistakes can be done if saturated permeabilities are introduced as input parameter in simulation softwares instead of effective values.

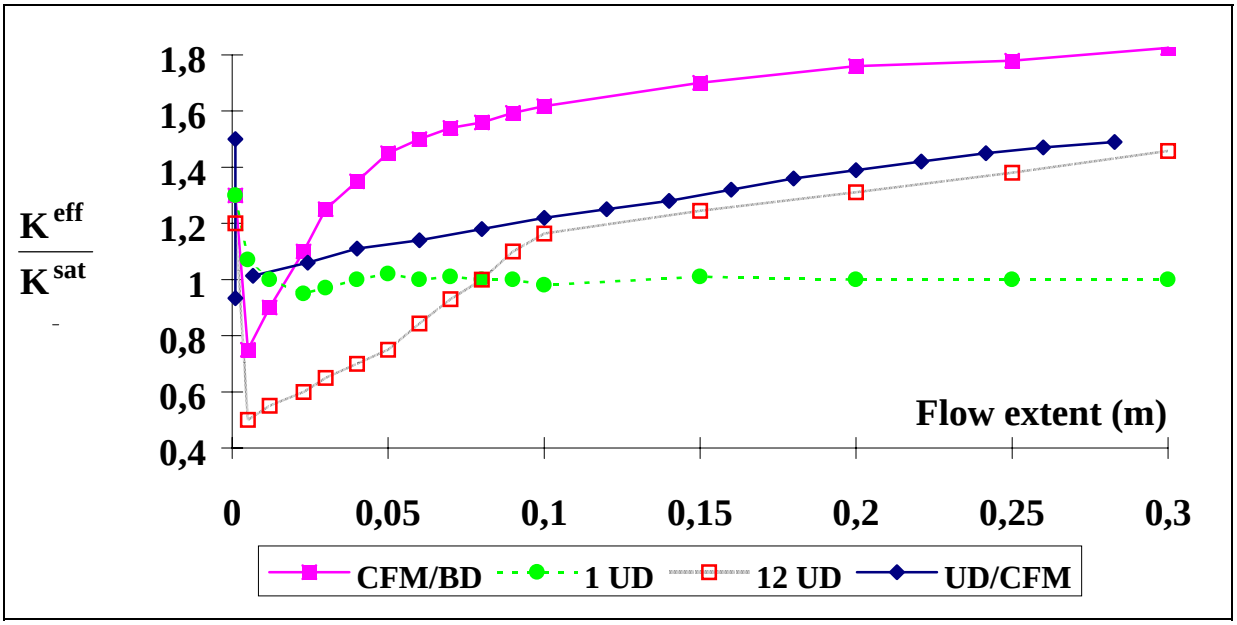

Fig.10 : Comparison of the experimental evolutions of the ratio K^{eff}/K^{sat} for the different reinforcements considered in this study

CONCLUSIONS

The aim of this work was to measure and to predict the effects of fabric architectural heterogeneities on effective and saturated permeabilities. Comparisons have been performed in terme of the dimensionless ratio K^{eff}/K^{sat}. Evolutions of this ratio are found to be related to the relative thickness and the transverse permeabilities of layers, the total length of the mold and the number of length scales embedded in preforms. An accurate geometric description of the fibrous network is needed to rebuild the actual flow path which is the less resistant path. Good qualitative and quantitative agreements are obtained, depending on the knowledge of the real pore size distribution . As a function of the time scales associated to local transverse flows, the proposed model predicts significant effects on effective permeabilities for thick and architecturally-complex materials. For these materials large molds are needed to fully characterize the flow behavior and to get steady-state values of effective permeabilities.

SYMBOLS

A_M	Macropores cross sectional area
A_m	micropores cross sectional area
e_{ij}	Distance between Macropores i and j in the transverse direction
K_m^t	Transverse permeability of tow
K_m^a	Axial permeability of tow
K_M	Inter-tow (Macropore) permeability
K^{eff}	Effective permeability
K^{sat}	Saturated permeability
P	Constant inlet pressure
Q	Volumetric flow rate
x	Transverse direction
z	In-plane flow extent
Δz	Lag distance in tows
μ	Viscosity

REFERENCES

1. Diallo M.L., Gauvin R. And Trochu F., "Key Factors Affecting The Permeability Measurement in Continuous Fiber Reinforcements", Proceedings of ICCM-11, Gold Coast, Australia, 14th-18th July, 1997, IV, pp. 441-451.

2. Luce T.L., Advani S.G., Howard J.G. and Parnas R.S., "Permeability Characterization. Part1 : A proposed Standard Reference Fabric for Permeability", Poymer Composites, Vol.16, No.6, 1995, pp. 429-445.

3. Parnas R.S. and Phelan F.R., SAMPE Q., "The Effect of Heterogeneous Porous Media on Mold Filling in Resin Transfer Molding", 1991.

4. Luce T.L., Advani S.G., Howard J.G. and Parnas R.S., "Permeability Characterization. Part2 : Flow behavior in Multiple-Layer Preforms", Poymer Composites, Vol.16, No.6, 1995, pp. 446-458.

5. Calado V.M.A. and Advani S.G., "Effective Average Permeability of Multi-Layer Preforms in Resin Transfer Molding", Composites Science and Technology, 56, 1996, pp. 519-531.

6. Binétruy C., Hilaire B. and Pabiot J., "Tow Impregantion Model and Void Formation Mechanisms during RTM", Journal of Composite Materials, Vol.31, No. 3, 1998, pp. 223-245.

7. Binétruy C., Hilaire B. and Pabiot J., "RTM Impregnation of High Fibre Content Composites : Modelization and Void Formation Mechanisms", Proceedings of the 16th SAMPE Europe Conference, Sazburg, Austria, May 30- June 1, 1995, pp. 345-355.

8. Binétruy C., Hilaire B. and Pabiot J., "The interactions between flows occuring inside and outside fabric tows during RTM", Composites Science and Technology, Vol.57, N°.6, 1997, pp. 587-596.

9. Binétruy C., Hilaire B. and Pabiot J., " A New Model for Preform Permeabilities Prediction and for Suitable RTM Reinforcements Design", Proccedings of the 18th SAMPE Europe Conference, Paris, La Défense, April 23-25, 1997, pp. 75-86.

10. Chan A.W., Morgan R.J., "Tow Impregnation during Resin Transfer Molding of Bidirectional Nonwoven Fabrics", Polymer Composites, Vol.14, N°.4, 1993.